Journal of Applied Polymer Science

Structural, Optical, and Conductive Properties of a Poly(styrene)-b-Poly(thiophene) Copolymer Doped with Fullerenes Under Different Conditions

Nikolaos Politakos,[1] Eftychia Grana,[2,3] Iñaki Zalakain,[1] Dimitrios Katsigiannopoulos,[2] Arantxa Eceiza,[1] Galder Kortaberria,[1] Apostolos Avgeropoulos[2]

[1]"Materials + Technologies" Group, Polytechnic School, Dpto. Ingeniería Química y M. Ambiente, Universidad País Vasco/Euskal Herriko Universitatea, Pza. Europa 1, 20018 Donostia-San Sebastian, Spain

[2]Department of Materials Science Engineering, University of Ioannina, University Campus, Ioannina 45110, Greece

[3]Laboratoire de Chimie des Polymères Organiques (LCPO) - UMR5629, Université Bordeaux, CNRS, IPB-ENSCBP, 16 Avenue Pey Berland, 33607 Pessac Cedex, France

Correspondance to: G. Kortaberria (E-mail: galder.cortaberria@ehu.es) and A. Avgeropoulos (E-mail: aavger@cc.uoi.gr)

ABSTRACT: In this manuscript mixtures of a poly(styrene)-b-poly(thiophene) (PS-b-PT) copolymer with fullerenes (C_{60}) as a dopant were prepared in order to evaluate their optical/surface properties through optical microscopy (OM) and atomic force microscopy (AFM) measurements respectively, as well as their conductivity through the four probe technique under variable conditions such as: temperature (room temperature and 150°C), solvent (toluene and chlorobenzene) and dopant concentration (2 and 5 wt %). The results exhibited that thermal treatment; solvent polarity and dopant concentration influence significantly the optical absorbance values. Ultraviolet-visible spectroscopy (UV-Vis) was also adopted to examine the optical absorbance of the mixtures and how it can be affected by the structures obtained in each case. The results for the variables involved in this study were very interesting and led to significant conclusions concerning the potential application of the proposed mixture for improved organic solar cells. © 2013 Wiley Periodicals, Inc. J. Appl. Polym. Sci. **2014**, *131*, 40084.

KEYWORDS: conducting polymers; copolymers; crystallization; optical and photovoltaic applications; optical properties

Received 12 August 2013; accepted 20 October 2013

DOI: 10.1002/app.40084

INTRODUCTION

As global energy consumption is constantly increasing, the quest for renewable and environmentally friendly resources is necessary in order to cover the energy needs maintaining low levels of carbon dioxide. Solar energy is one of the most important renewable energy sources and it is currently applied by the use of various types of solar cells.[1] Although, the solar cells market is overwhelmed from inorganic materials, new approaches concerning organic solar cells are under investigation and fabrication since they present important properties (environmental safety, low cost, efficiency, flexibility, and low weight), leading to strong potential infiltration in the solar cell market.

There are three types of organic solar cells with satisfactory efficiencies: (1) Dye-sensitized solar cells, in which an organic dye is adsorbed at the surface of an inorganic wide band semiconductor (e.g., ruthenium dye-sensitized nanocrystalline TiO_2 (nc-TiO_2) solar cells, with an efficiency of ~10%);[2–4] (2) double layer cells, for which the formation of a double layer structure of a *p*- and *n*-type organic semiconductor is requested,[5,6] and (3) bulk heterojunction cells, (BHJ), for which a combination of an electron donating (*p*-type) and an electron accepting (*n*-type) materials is used in the active layer. Excitons created in all cases must diffuse on the interface to enable charge separation. Polymer-fullerene solar cells were among the first materials applied in the aforementioned type III organic solar cells.[7] These materials should be preferably mixed into a bicontinuous interpenetrating network in order to achieve higher efficiency. It should be mentioned that polymeric heterojunctions can exhibit different architectures, such as: (a) bilayer (with limitations, due to the active layer length), (b) bulk heterojunction, and (c) ordered heterojunction.[8]

Organic solar cells are considered as low cost alternative materials with mechanical flexibility[9–12] and potential variation of their bandgap through the incorporation of different polymers,

in order to harvest more efficiently the solar spectrum.[10,11] Poly(thiophene) is one of the most applied polymers for organic solar cells,[13] since it presents desirable optical properties, thermal, and environmental stability with potential applications on electronics, photovoltaics, sensors, and transistors.[14,15] Unfortunately, the low solubility of poly(thiophene) in most organic solvents has led to the use of either substituted poly(thiophenes) or block copolymers with poly(thiophene) as one of the blocks.

Block copolymers present very interesting properties which are directly connected with their chemical structure and architecture. The manner through which different segments are linked together and the adopted periodic microstructures leading to well-ordered nanodomains through direct self-assembly have already been reported in the literature.[16–18] Furthermore, the use of graft copolymerization of thiophene onto polystyrene (PS) chains or poly(ethylene) surfaces has already been reported as a way to combine conventional polymers (e.g., PS) with poly(thiophene).[19,20]

Mobility of charge-carriers (which is the key for increased efficiency of a solar cell) is affected by different parameters such as molecular and morphological structure of the organic layers,[12,21] crystallinity and microstructure (always described by the local molecular ordering, domain size, and formation of percolating structures).[12] In order to achieve satisfactory performance for a solar cell many different parameters should be taken into account for optimizing the results. The generation of a three-dimensional photoactive matrix with a large charge generation interface is crucial as already reported.[10,11] Crystallinity, in combination with domain size, also affects the properties and efficiency of solar cells.[12,22] Optimization of the molecular weight may lead to better results, since it is considered important for the processing and performance of the active layers.[12] Solvent, composition, and thermal treatment[10,11,23,24] have also shown a great impact on the cell efficiency.

For BHJ solar cells, the best properties have been reported for those pairs which include a polymer and a fullerene derivative. Concerning the polymer part, different chemical structures such as poly(3-hexylthiophene) or P3HT,[10–12,25] substituted thieno compounds,[26] and poly(phenylene vinylene) or PPV[27,28] have been used. In the case of fullerene derivatives the most commonly used is $PC_{61}BM$ (phenyl-C_{61}-butyric acid methyl ester),[10,11,25,29,30] but also others such as $PC_{70}BM$[9,26] and simple C_{60}.[27,28] Intercalation of fullerenes among the polymer chains has led to satisfactory results.[26,29,30] The formation of percolated pathways from the fullerene phase in order to achieve holes and electron transport is very important[24] since it is considered to be highly related to the generated microstructure and/or nanostructure as well as to the applied conditions and it is affected by the manner the fullerene phase is separated from the corresponding polymer. It has been reported that the use of chlorobenzene as solvent may lead to improved behavior increasing overall efficiency, together with the generation of smoother surfaces eventually enhancing the charge carrier mobility.[29,30]

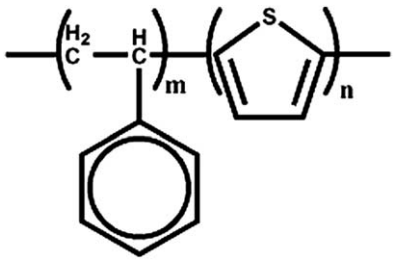

Figure 1. Chemical structure of the PS-b-PT [poly(styrene)-b-poly(thiophene)] diblock copolymer.

The present research work involves the evaluation of structural and surface properties of a poly(styrene)-b-poly(thiophene) (PS-b-PT) copolymer, doped with different concentrations of fullerenes (C_{60}) (2 and 5 wt %), taking into account the effect of variable solvent and temperature treatment. For the specific PS-b-PT copolymer, its optical, conductive and surface properties have not been excessively reported in the literature, neither for the raw material, nor for its composites with carbon structures such as nonsubstituted fullerenes which is the major focus of our study. It should be mentioned though that a relative study has been reported recently in which a similar diblock copolymer was incorporated with the difference on the PT segment; being a substituted PT and specifically poly(3-hexylthiophene).[31]

EXPERIMENTAL

Materials

The copolymer used for this study was PS-b-PT which has been synthesized with a procedure already reported in the literature.[32–34] The chemical structure of the copolymer can be seen in Figure 1, while its molecular characteristics, measured by size exclusion chromatography (SEC) and membrane osmometry (MO) are listed in Table I. Polythiophene is chemically bonded to a common soluble block (PS), exhibiting molecular homogeneity (polydispersity index: I<1.1). PS chains increase the solubility and processability in common organic solvents (e.g., toluene, xylene, tetrahydrofuran, chloroform, and chlorobenzene) when compared to pure PT. Unsubstituted PT was used as one block of the copolymer since, as reported in the literature,[32–34] substituted PT derivatives lead to significant decrease of the electrical properties. Fullerene (C_{60}), used in the donor-acceptor pair together with PS-b-PT, was purchased from Aldrich (98% purity). Toluene (Lab Scan, HPLC, 99%) and chlorobenzene (Panreac, 99.5%) were used as solvents for preparing the studied mixtures.

Table I. Molecular Characteristics of PS-b-PT Copolymer

Copolymer	$(\overline{M}_n)_{PS}$ [a] g/mol	$(\overline{M}_n)_{PT}$ [b] g/mol	$(\overline{M}_n)_{tot}$ [a] g/mol	I[c]	f (PS) [d]
PS-b-PT	98,000	12,000	110,000	1.02	0.89

[a] Membrane osmometry (MO) in toluene at 35°C.
[b] $(\overline{M}_n)_{PT}=(\overline{M}_n)_{tot}-(\overline{M}_n)_{PS}$.
[c] Size exclusion chromatography (SEC) in THF at 35°C.
[d] Mass fraction directly calculated from molecular weights.

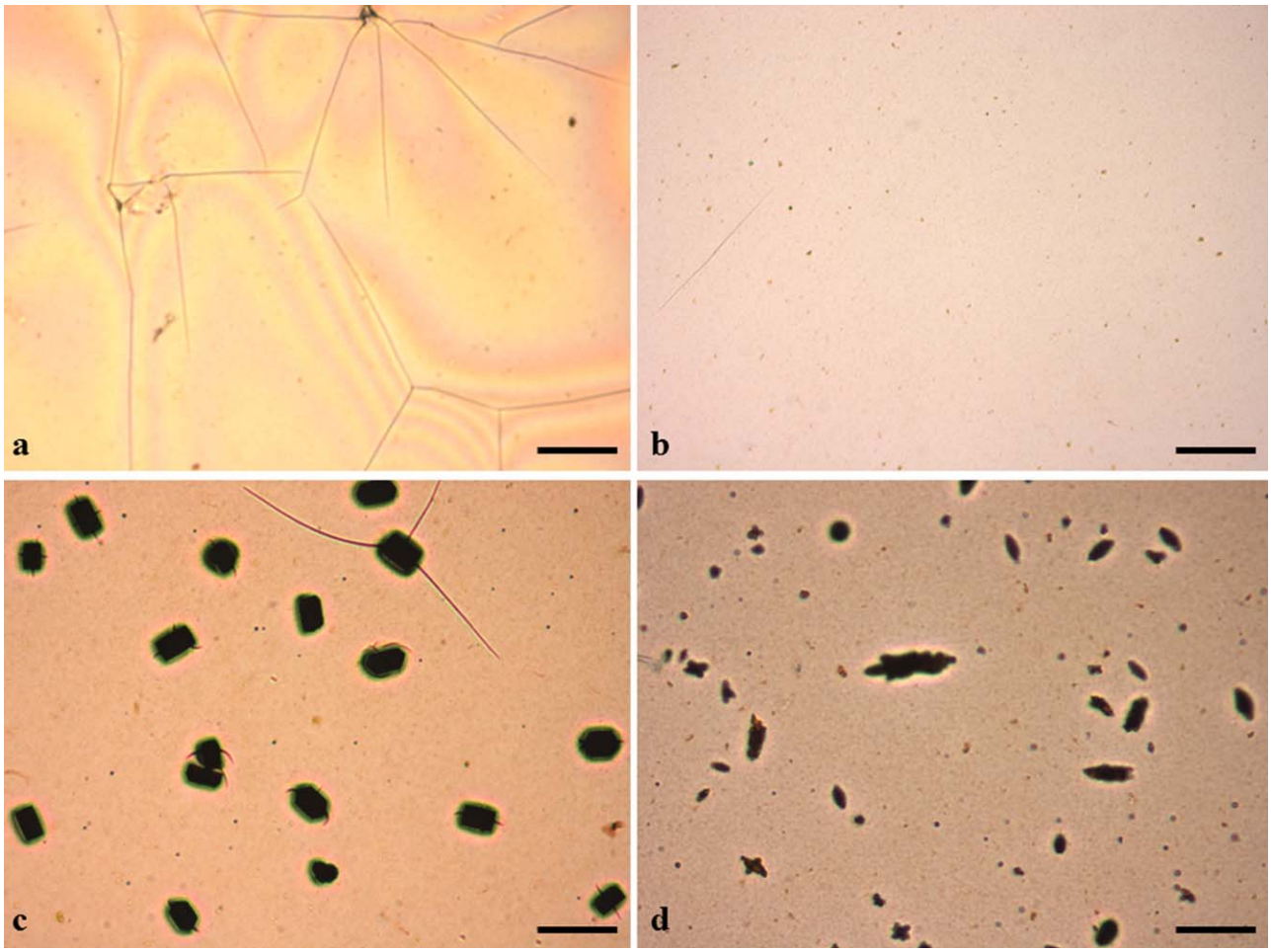

Figure 2. Optical microscopy images (x50 magnification) of the mixtures at room temperature with C_{60} wt % concentration for: (a) 2 wt % in toluene, (b) 2 wt % in chlorobenzene, (c) 5 wt % in toluene, and (d) 5 wt % in chlorobenzene. The scale bar in all images corresponds to 200 μm. [Color figure can be viewed in the online issue, which is available at wileyonlinelibrary.com.]

Preparation of PS-b-PT/C_{60} Mixtures

Prior to the mixture preparation, fullerenes were dried under vacuum (100°C) in order to remove possible humidity traces. For PS-b-PT, 10% w/w solutions were prepared in toluene, while for fullerenes 3 mg/mL solutions were prepared in different solvents (toluene and chlorobenzene) under stirring for 24 h at room temperature. Before mixing both solutions, the fullerenes solution was sonicated in a water bath, for 2 h at ambient conditions. Two different concentrations were chosen for fullerenes in relation to the copolymer: 2 and 5 wt %, respectively. Both solutions were then mixed and stirred for 24 h at room temperature followed by sonication for 1 h. Then samples were cast into glass wafers for solvent evaporation. Some of them were then annealed at 150°C in order to check the effect of thermal treatment. The main goal was to evaluate differences in the absorption for different concentrations and to analyze how the structures obtained at room temperature and after annealing could affect surface and electrical properties.

Characterization

For ultraviolet-visible spectroscopy (UV-Vis) measurements a UV-3600 Shimadzu UV-VIS-NIR spectrophotometer was used with a scan range from 200 to 800 nm, and equipped with an optical path quartz cuvette of 1 cm.

For optical microscopy (OM) characterization a Nikon Eclipse E600 microscope was used. Atomic force microscopy (AFM) was performed with a Veeco Dimesion Icon (from Digital Instruments). Tapping mode in air was employed using an integrated silicon tip/cantilever (125 μm in length and with ca. 300 kHz resonant frequency) at a scan rate of 1.0 Hz and a resonance frequency of ~300 kHz. For electrical characterization 4200-SCS Keithley equipment was used in four-probe mode to measure sheet resistivity (ρ), which is directly connected with conductivity ($\sigma = 1/\rho$).

RESULTS AND DISCUSSION

Optical Microscopy

Optical microscopy (OM) was used as a primary tool in order to observe phase separation between PS-b-PT and C_{60} and have an initial image of the structure adopted. A series of samples with different C_{60} concentrations prepared in different solvents and under variable temperatures (room temperature and 150°C) were used. In Figure 2, OM images of 2 and 5 wt % of

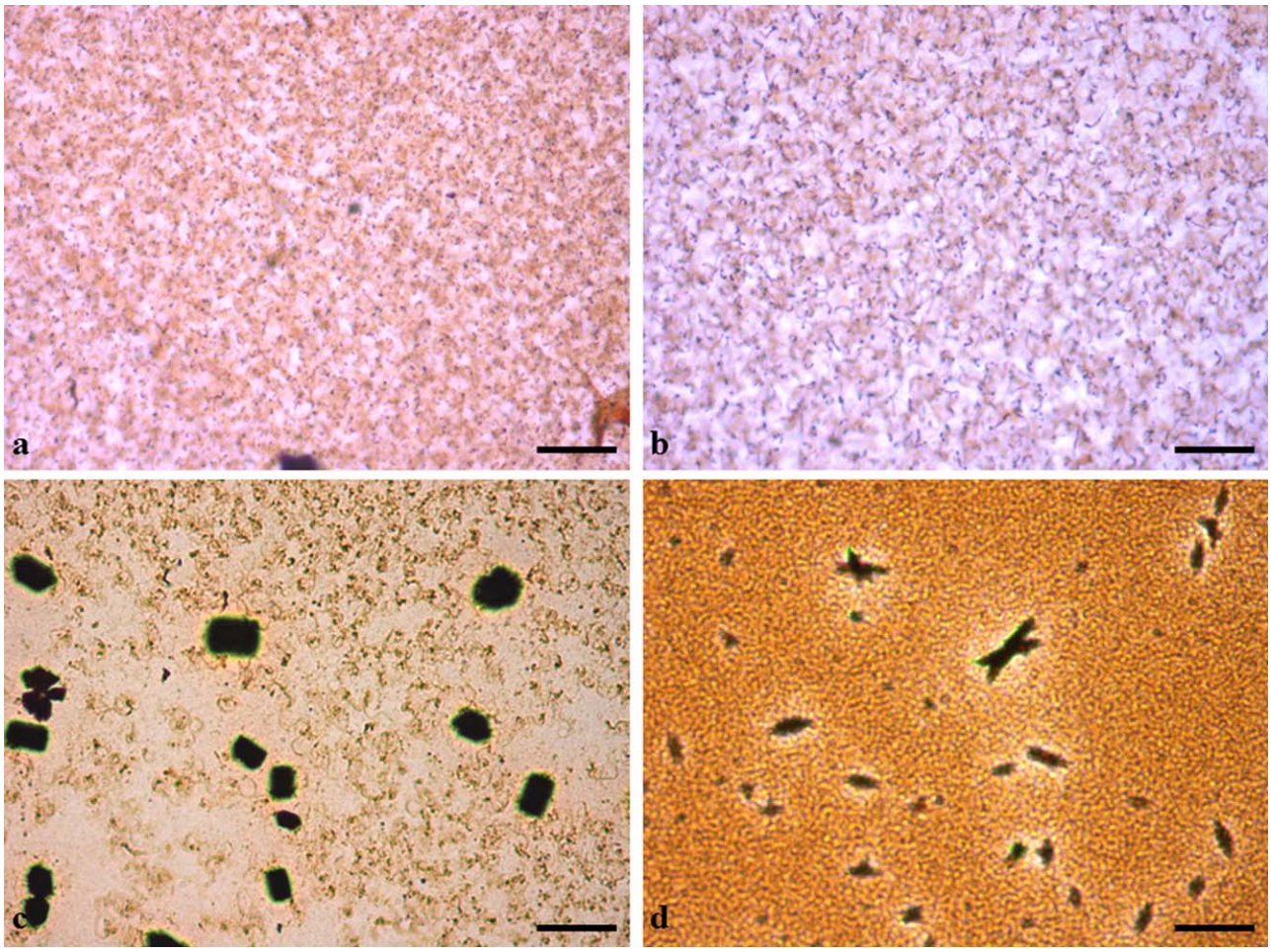

Figure 3. Optical microscopy images (x50 magnification) of the mixtures annealed at 150°C with C_{60} wt % concentration for: (a) 2 wt % in toluene, (b) 2 wt % in chlorobenzene, (c) 5 wt % in toluene, and (d) 5 wt % in chlorobenzene. The scale bar in all images corresponds to 200 μm. [Color figure can be viewed in the online issue, which is available at wileyonlinelibrary.com.]

C_{60} prepared with both solvents at room temperature can be observed. It is evident that the 2 wt % in C_{60} samples did not show any phase separation, neither any structural difference [Figure 2(a,b)].

From Figure 2(c,d), it can be observed that for samples with 5 wt % in C_{60}, some crystalline domains were generated ascribed to the increased fullerene content and their crystalline nature. It must be noted that, in the case of samples prepared with toluene, the polydispersity of the domains is much higher than that of samples prepared with chlorobenzene.[23] Systems containing fullerene derivatives and poly(thiophene) as the basic polymer conductive material exhibited crystallinity for both components. For poly(thiophene) itself a crystallinity degree of ~35% at room temperature has been observed, which is increased up to 52% by annealing at high temperatures,[35,36] leading eventually to low device performance as it has been observed for similar systems with substituted poly(thiophenes) and fullerenes.[37–41] In contradiction, at room temperature the crystalline phase of the fullerenes affected the overall macrophase separation for these systems.

In Figure 3 optical microscopy images for samples prepared with both toluene and chlorobenzene and annealed for 24 h at 150°C can be seen. Table II summarizes the obtained structures

Table II. Structural Surface Characteristics of PS-b-PT/C_{60} Thin Films as Obtained from Optical Microscopy

Sample	Room temperature	Annealed at 150°C
	Structure	
PS-PT/C_{60}_TOL (2%)	–	Spiral tube network
PS-PT/C_{60}_CB (2%)	–	Spiral tube network
PS-PT/C_{60}_TOL (5%)	Polygonal fullerene crystals	Spiral tube network. Polygonal fullerene crystals
PS-PT/C_{60}_CB (5%)	Needle-shape fullerene crystals	Small fullerene domains. Needle-shape fullerene crystals

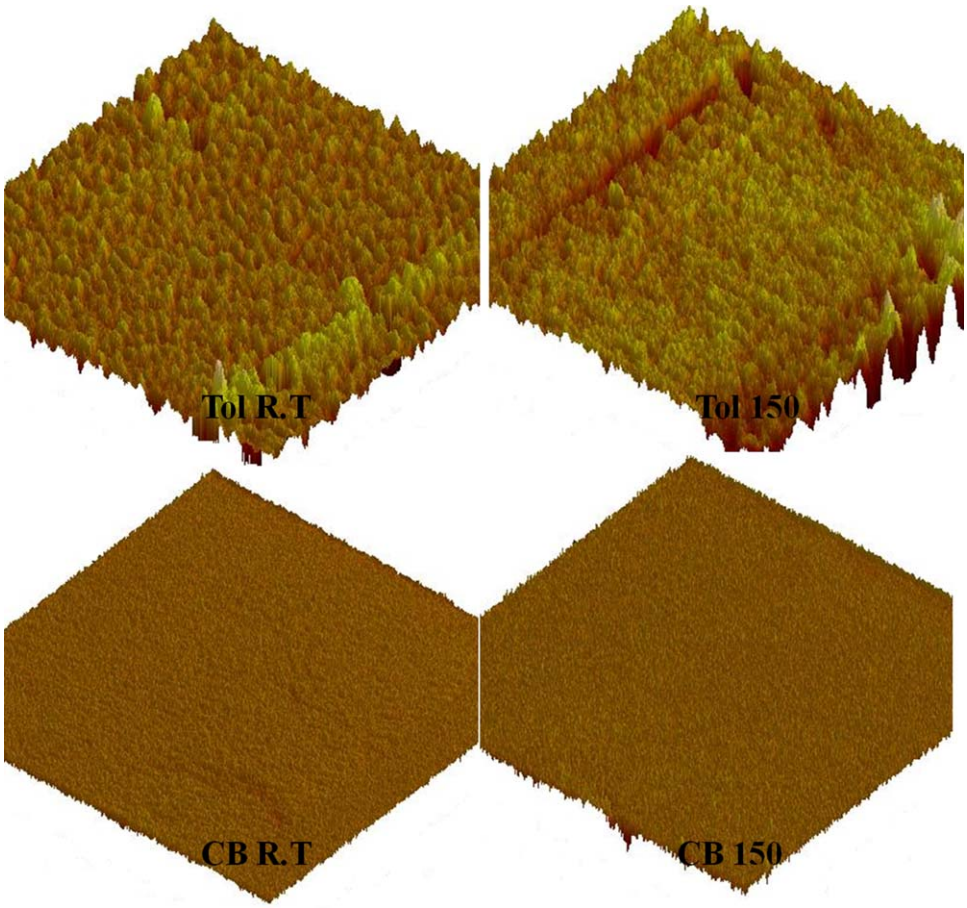

Figure 4. Phase AFM images (1μm x 1μm) for 2 wt % of fullerenes, prepared with both solvents, before and after thermal treatment. [Color figure can be viewed in the online issue, which is available at wileyonlinelibrary.com.]

and phase behavior of all samples. In the case of the materials with 2 wt % in C_{60} the results were quite similar for both solvents leading to the observation of spiral tubes. For mixtures with 5 wt % in C_{60}, phase separation can be observed exhibiting different structures for the C_{60} phase which seem to depend on the nature of the solvent. For samples prepared in toluene, small spiral tubes with big fullerene domains were observed, as already mentioned in the literature[37,39] for similar systems. For the chlorobenzene case the morphology of the structural domains seems to be more needle-shaped.

For samples with higher C_{60} concentration and thermal treatment, a 2D network is formed with needle-shape aggregated domains which, unfortunately, led to low device performance.[37–41] At higher temperatures, fullerene can diffuse inside the film and, together with poly(thiophene) mobility, crystalline domains can be created with the fullerenes being shaped as needles.[38,39] The needle like shape crystals appeared to be more evident at higher temperatures and were transferred on to the air surface, thus resulting to larger needles.[42,43] In the annealed samples with 2 wt % C_{60} prepared in toluene similar homogeneity was observed, which is altered for those with 5 wt % C_{60}, where polygonal domains coexist with a spiral tube network. In addition, for the samples prepared in chlorobenzene, the matrix appears more homogeneous when compared with those prepared in toluene, where it is evident that the polygonal large domains were substituted by needle-shape smaller ones. It is concluded therefore, that solvent and especially solvent polarity is a key parameter responsible for the surface morphologies obtained, whereas, thermal treatment assisted the C_{60} to migrate onto the surface.

Atomic Force Microscopy (AFM)

This technique was used in order to evaluate the evolution of topography and the phase roughness with thermal treatment (24 h at room temperature and at 150°C) and solvent polarity. From AFM images the range in nm and ° hardness for height and phase images respectively was studied, together with the roughness R_{ms} in nm and ° for both height and phase images. Figures 4 and 5 show 3D phase images for mixtures with 2 and 5 wt % in fullerenes, whereas, the results from all the aforementioned parameters are summarized in Table III.

It is evident that thermal treatment and solvent polarity affect the range and roughness of the samples. Generally, the increase in polarity leads to a substantial decrease in range order. It has already been reported that chlorobenzene tends to suppress the fullerenes behavior into forming clusters.[24,29,30] From Figures 4 and 5 and Table III results for range, it can be concluded that for samples with 2 wt % in C_{60} the changes in range by altering

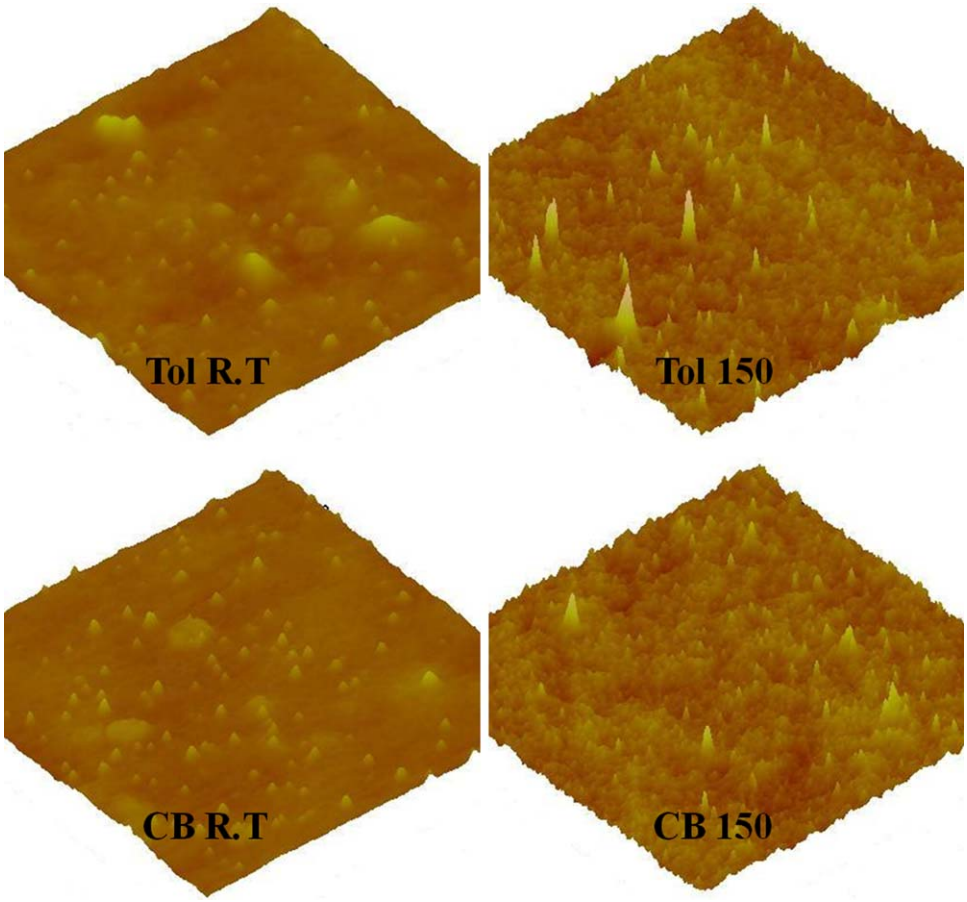

Figure 5. Phase AFM images (1μm x 1μm) for 5 wt % of fullerenes, prepared with both solvents, before and after thermal treatment. [Color figure can be viewed in the online issue, which is available at wileyonlinelibrary.com.]

the temperature are minimal whereas a completely controversial behavior is evident for the corresponding 5 wt % case.

Results are similar for the roughness parameter, leading to the conclusion that roughness[44] and aggregation are enhanced by increasing the fullerene concentration (especially for variable time and different annealing temperatures, roughness is also increased as reported in the literature[40,41]). Roughness is increased through solvent polarity.[45] Increased wt % in C_{60} leads to less smooth surfaces with relatively enhanced roughness (in nm and in °). The thermal treatment concluded to rougher surfaces due to possible migration of the fullerenes onto the outer surface. The nature of the solvent affects the manner in which fullerenes diffuse in each composite material and crystallize. Also, the fact that the amorphous PS soft phase affects diffusion of fullerenes and roughness after the thermal treatment must be considered. In Figures 4 and 5 more homogeneous phases with less aggregation levels and roughness for samples prepared in chlorobenzene can be observed. It seems that toluene leads to increased aggregation, larger domains and rougher surfaces when compared with the polar chlorobenzene.

Table III. Range and Roughness Values (from Height and Phase) for Samples with 2 and 5 wt % of Fullerenes as Obtained from AFM

Sample	Range (nm) Height	Rms (nm) Height	Range (°) Phase	Rms (°) Phase
2% Tol R.T.	6-12	0.64	14-39	2.88
2% Tol ann	5-14	0.63	13-20	3.38
2% CB R.T.	4-12	0.58	4-13	1.22
2% CB ann	5-11	0.66	4-12	1.38
5% Tol R.T.	4-18	0.81	22-42	3.02
5% Tol ann	2-20	1.00	11-45	3.52
5% CB R.T.	4-15	0.72	11-21	2.15
5% CB ann	5-16	0.89	15-35	2.91

Ultraviolet-Visible (UV-Vis) Spectroscopy

Figure 6 involves the UV-Vis spectra for neat copolymer films prepared at room temperature and after thermal annealing at 150°C, together with those corresponding to neat fullerene solutions prepared in toluene and chlorobenzene. For the neat C_{60} solutions optical absorptions are exhibited at ~364, 371, 389 nm with another broad absorption at 600 nm in complete agreement with the literature.[46] Concerning the total optical absorption, C_{60} solutions in chlorobenzene present higher

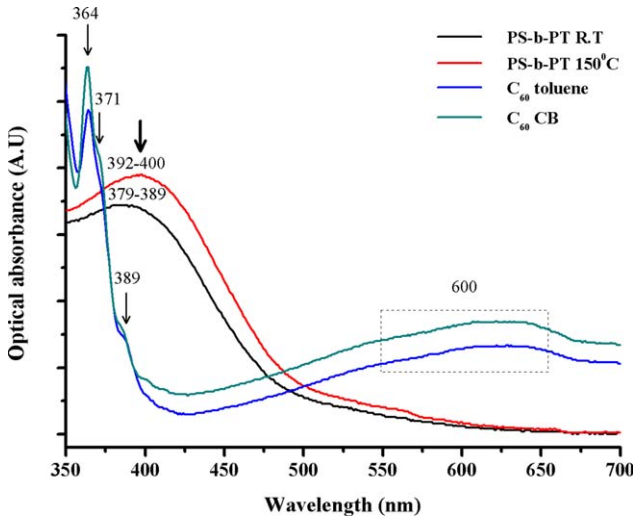

Figure 6. Optical absorbance for the neat PS-b-PT copolymer films at room temperature and after annealing as well as for the respective fullerene solutions in toluene and chlorobenzene, as measured by UV-Vis spectroscopy. [Color figure can be viewed in the online issue, which is available at wileyonlinelibrary.com.]

absorption than those in toluene. As the π^* state is considered polar, π-π^* transitions are more favorable for polar solvents.

For the neat PS-b-PT copolymer a maximum between 379 and 389 nm can be observed for the sample prepared at room temperature and between 392 and 400 nm for the annealed one. In the latter case a small absorption can be seen at ~560 nm. For both temperatures the optical absorption starts to faint at ~500 nm. For the copolymer a bathochromic effect was observed after annealing (red shift to lower energy), probably due to the crystallization process of the PT block. The shifting of the maximum peak towards larger wavenumbers could be due to the fact that lower energy is required for exciting electrons, because of their ability to delocalize resulting from conjugation. For the PT chains, π-π^* transition maximum depends on the mean conjugation length of the backbone, which can be altered by annealing.[47]

Figure 7 exhibits the results from UV-Vis spectroscopy for mixtures prepared in toluene and chlorobenzene, under different fullerene concentrations, with and without thermal annealing. As it can be seen, solvent polarity, thermal treatment and concentration affects the position and the intensity of the observed peaks. The most intense transitions for all samples are summarized in Table IV.

From Figure 7 and Table IV, useful conclusions can be extracted related with the optical absorbance and the position of different peaks by changing preparation parameters. From Figure 7, three distinct peaks are evident in almost all cases, at 417, 476, and 667 nm respectively, with the one at 417 nm being the most prominent. Enhancement of optical absorption is also observed through the appearance of a broad peak at the region 400–550 nm.

In the cases where nonpolar toluene is used, it seems that by increasing temperature or concentration of the dopant the total optical absorption is decreased. In addition, chlorobenzene samples showed exactly the opposite behavior. It is clear that optical absorption is enhanced by increasing temperature, probably due to the higher aggregation level of fullerene, as it has been seen for similar systems with fullerenes.[45] It is also evident that the formation of the crystalline phase (and its size and form) of fullerenes and the aggregation degree is affected predominantly from the nature of the solvent, leading eventually to higher (case of chlorobenzene) or lower (case of toluene) optical absorptions. It should also be noted that the optical absorption of all mixtures is significantly enhanced when compared to those of pure PS-b-PT copolymer and fullerenes.

The different peaks observed in the spectra are directly attributed to the π-π^* transitions due to incorporation of C_{60} among the polymer chains. The transitions at 417 and 667 nm, respectively, which are present in all samples, are linked with the fullerene presence, being almost identical with those transitions exhibited in the pure fullerene spectra respectively. The intense peak at 476 nm is probably a new transition generated by the fullerene doping into the PS-b-PT copolymer. The peak at 667 nm is observed only for the annealed prepared in toluene samples as well as for the 2 wt % sample prepared in chlorobenzene, probably due the incorporation and aggregation of C_{60}.

Comparing the peaks at 417 nm and 667 nm of mixtures with those of neat C_{60} a bathochromic effect (red shift) is found, which could be due to structural changes. This effect is favored by polar solvents (chlorobenzene) and by fullerene aggregation (favored by increased temperature and fullerene concentration). This red shift is also connected with a J-aggregation (where molecule arrangements are aligned parallel to their centers) and needs less energy. By increasing concentration this aggregation is hindered, therefore, the interactions between the C_{60} molecules are being decreased.[44] The extent of this shift is related to strong chain-chain interactions since, after thermal treatment, intermolecular interactions inside the aggregates, favored by the nature of the crystal are evident.[48] By increasing temperature and concentration, the peak intensity is enhanced only for samples prepared in chlorobezene, while toluene environment leads to lower values. Fullerenes present an extended 2D π electron system which is strongly overlapping with the block copolymer in the mixtures. They also exhibit large electron affinity and can quickly capture electrons, a behavior which explains why they are considered as one of the best candidates for solar cells applications.[49,50] In these systems most transitions are attributed to π-π^* interactions[39,51,52] and are favored by polar environment and high degree of delocalization (higher conjugation and lower energy). Therefore, the idea of a J-aggregation (a relative loose one) of the polymer blocks (due to the presence of C_{60}) is extracted from the aforementioned results together with the fact that it can be achieved with considerably lower energy.

Conductivity Results

Conductivity of these samples is affected from different parameters, such as crystallization process which occurs after annealing, especially for the fullerenes. The different solvents (toluene and chlorobenzene) have also a great effect on the conductivity,

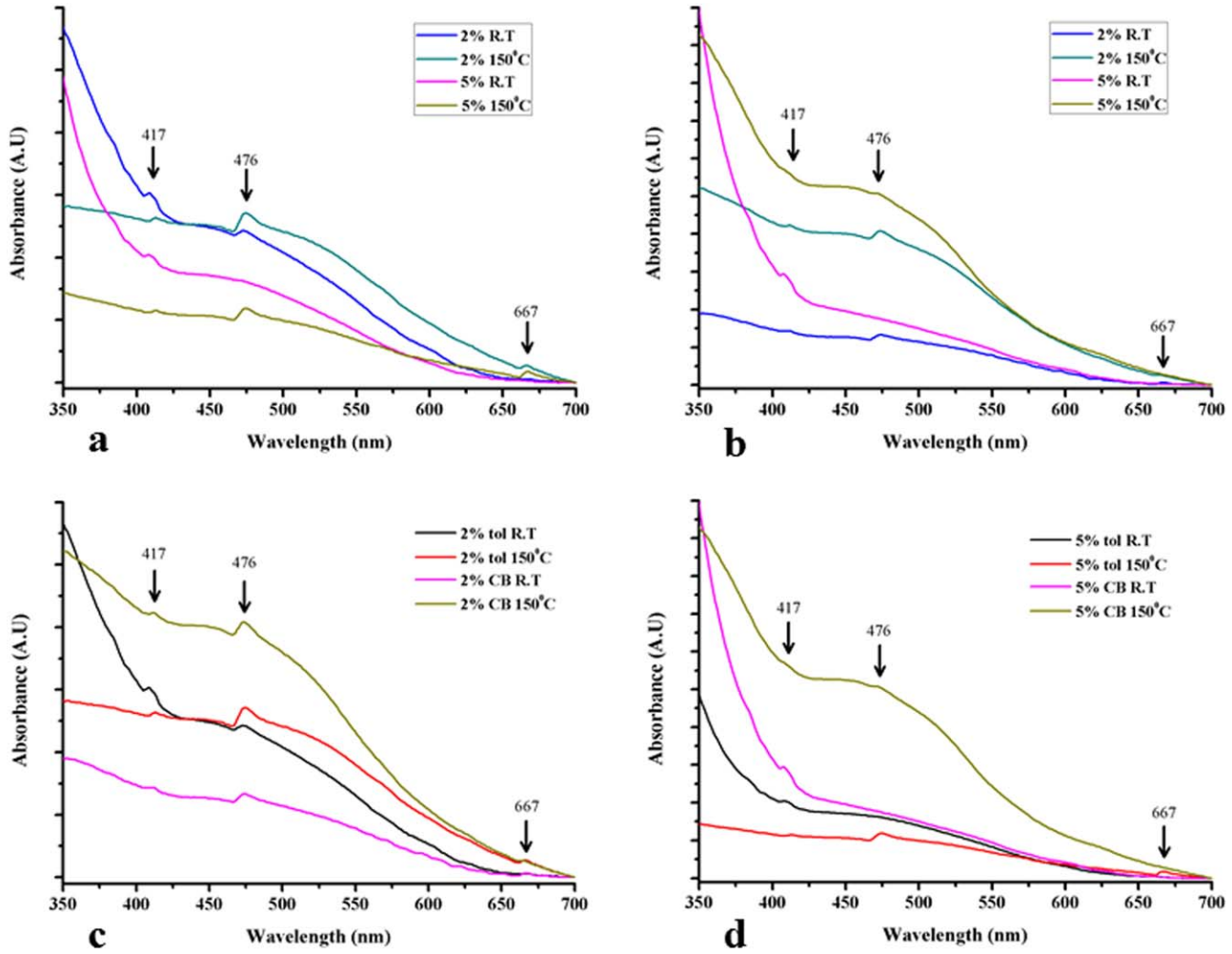

Figure 7. Optical absorbance for PS-b-PT/C_{60} thin films for (a) 2 and 5 wt % for toluene, (b) 2 and 5 wt % for chlorobenzene, (c) 2 wt % of all mixtures, and (d) 5 wt % of all mixtures, as measured by UV-Vis spectroscopy for both temperatures (R.T. and 150°C respectively). [Color figure can be viewed in the online issue, which is available at wileyonlinelibrary.com.]

since different domains in size and form can be created depending also on the different mixtures (concentration of the fullerenes and temperature). In Table V the sheet conductivity is presented for all aforementioned systems.

From the results different tendencies on conductivity depending on the concentration of the fullerenes, the solvent and the temperature of annealing can be observed. The conductivity of different systems varies from 4.41 mS/cm up to 7.45 mS/cm. By increasing the dopant concentration the conductivity decreases, probably due to the fact that the higher amount of fullerenes can distort the polymeric chains, affecting the charge transfer among polymer and dopants. Several research groups have reported that beyond a dopant concentration the conductivity was not higher or even decreased.[53,54] Interchain and intrachain charge transfer respectively is distorted from the relatively large size of the dopant.[55–58] Regarding the solvent effect, it is observed that chlorobenzene is leading to higher conductivity values in comparison to toluene, due to different size, form and aggregation degree of the domains which are created. Finally, the annealing treatment increased conductivity values when compared with samples studied at room temperature.

Table IV. Appearance of the Most Important Peaks for PS-b-PT/C_{60} Mixtures with Different Concentrations, Solvents, and Temperatures

Sample	*Peak A R.T	*Peak B R.T	*Peak C R.T	*Peak A ann	*Peak B ann	*Peak C ann
TOL (2%)	γ	γ	–	γ	γ	γ
CB (2%)	γ	γ	γ	γ	γ	Weak
TOL (5%)	γ	–	–	γ	γ	γ
CB (5%)	γ	–	–	Weak	Weak	–

*Peak A appears at 417 nm, peak B appears at 476 nm and peak C appears at 667 nm.

Table V. Coductivity Results for Samples with 2 and 5 wt % of Fullerenes Prepared with Both Toluene and Chlorobenzene at Room Temperature and After Thermal Treatment. In all case the sample thickness was approximately 0.003 cm.

Sample	*σ (mS/cm)
2% TOL R.T	4.47
2% TOL ann	6.64
2% CB R.T	6.35
2% CB ann	7.45
5% TOL R.T	4.41
5% TOL ann	5.30
5% CB R.T	4.42
5% CB ann	6.28

*$\sigma=1/\rho$, ρ(sheet resistivity). Sheet resistivity is calculated from the four probe method.

CONCLUSIONS

For PS-b-PT/ C_{60} mixtures the main target was to evaluate the optical properties and to analyze how the final composite surface is affected by temperature, C_{60} concentration, and solvent polarity. From the analysis of the surface via optical microscopy and AFM, interesting results were found for the aggregation of the fullerenes and how it affects the roughness of the surface, as well as for the size and form of the crystallites generated due to higher fullerene concentration and thermal treatment. Annealing concluded to the fact that, fullerenes migrate to the surface of the sample, creating a network at 2 wt % in C_{60} concentration, whereas at 5 wt % in C_{60} this network is more homogeneous for the chlorobenzene prepared samples. The shape and size of fullerene crystals is quite different in the two solvents used for this study. Furthermore, roughness is enhanced for toluene samples, an observation which is also evident at higher temperature and higher wt% of C_{60}. The optical properties are directly related with the concentration of the fullerenes, temperature, and solvent polarity. The appearance of a transition at 476 nm could be connected with interactions between fullerenes and PS-b-PT, after incorporation of the dopant into the polymeric matrix. Finally, a decrease in sheet conductivity was evident when the fullerene content increased as well as in the annealed samples and when the solvent polarity increased, probably due to distortion produced in the polymeric chains, affecting the charge transfer among polymer and dopants.

ACKNOWLEDGMENTS

Financial support from the Basque Country Government (Nano-Iker IE11-304, SAIOTEK2012-S-PE12UN106, Grupos Consolidados IT776-13) and from the Ministry of Education and Innovation (MAT2012-31675) is gratefully acknowledged. Technical and human support provided by SGIker (UPV/EHU, MICINN, GV/EJ, ERDF and ESF) is also acknowledged.

REFERENCES

1. Jager-Waldau, A. *PV Status Report* **2003** 2003, European Commission, EUR 20850 EN.
2. Regan, B. O.; Gratzel, M. *Nature* **1991**, *335*, 737.
3. Nazeeruddin, M. K.; Réchy, P.; Renouard, T.; Zakeeruddin, S. M.; Humphry-Baker, R.; Comte, P.; Liska, P.; Vevey, L.; Costa, E.; Shklover, V.; Spicca, L.; Deacon, G. B.; Bignozzi, C. A.; Gratzel, M. *J. Am. Chem. Soc.* **2001**, *123*, 1613.
4. Malekshahi Byranvand, M.; Nermati Kharat, A.; Bazargan, M. H. *Nano-Micro Letters* **2012**, *4*, 253.
5. Chamberlain, G. A. *Solar Cells* **1983**, *8*, 47.
6. Tang, C. W. *Appl. Phys. Lett.* **1986**, *48*, 183.
7. Yu, G.; Gao Y.; Hummelen, J. C.; Wudl, F.; Heeger, A. *J. Science* **1995**, *270*, 1789.
8. Mayer, A. C.; Scully, S. R.; Hardin, B. E.; Rowell, M. W.; McGehee, M. D. *Materials Today* **2007**, *10*, 28.
9. Tang, Y.; McNeill, C. R. J. Polym. Sci., *Part B: Polym. Phys.* **2013**, *51*, 403.
10. Padinger, F.; Rittberger, R. S.; Sariciftci, N. S. *Adv. Funct. Mater.* **2003**, *13*, 85.
11. Engmann, S.; Turkovic, V.; Denner, P.; Hoppe, H.; Gobsch, G. J. Polym. Sci., *Part B: Polym. Phys.* **2012**, *50*, 1363.
12. Brabec, C. J.; Heeney, M.; McCulloch, I.; Nelson, J. *Chem. Soc. Rev.* **2011**, *40*, 1185.
13. Perrin, L.; Nourdine, A.; Planes, E.; Carrot, C.; Alberola, N.; Flandin, L. J. Polym. Sci., *Part B: Polym. Phys.* **2013**, *51*, 291.
14. Vatansever, F.; Hacaloglu, J.; Akbulut, U.; Toppare, L. *Polymer International* **1996**, *41*, 237.
15. Erdonmez, S.; Ozkazanc, E. *Polym. Int.* **2013**, DOI *10*.1002/pi.4536.
16. Kimishima, K.; Jinnai, H.; Hashimoto, T. *Macromolecules* **1999**, *32*, 2585.
17. Tureau, M. S.; Epps, T. H. *Macromolecules* **2012**, *45*, 8347.
18. Topham, P. D.; Parnell, A. J.; Hiorns, R.C. J. Polym. Sci., *Part B: Polym. Phys.* **2011**, *49*, 1131.
19. Hatamzadeh, M.; Jaymand, M.; Massoumi, B. *Polym. Int.* **2013**, DOI *10*.1002/pi.4513.
20. Chanunpanich, N.; Ulman, A.; Strzhemechny, Y. M.; Schwarz, S. A.; Dormicik, J.; Janke, A.; Braun, H. G.; Kratzmuller, T. *Polym. Int.* **2003**, *52*, 172.
21. Brédas, J. L.; Norton, J. E.; Cornil, J.; Coropceanu, V. *Acc. Chem. Res.* **2009**, *42*, 1691.
22. Chochos, C. L.; Choulis, S. A. *Prog. Polym. Sci.* **2011**, *36*, 1326.
23. Chen, L. M.; Hong, Z.; Li, G.; Yang, Y. *Adv. Mater.* **2009**, *21*, 1434.
24. Hoppe, H.; Sariciftci, N. S. *Adv. Polym. Sci.* **2008**, *214*, 1.
25. Tada, A.; Geng, Y.; Wei, Q.; Hashimoto, K.; Tajima, K. *Nat. Mater.* **2011**, *10*, 450.
26. Cates, N. C.; Gysel, R.; Beily, Z.; Miller, C. E.; Toney, M. F.; Heeney, M.; McCulloch, I.; McGehee, M. D. *Nano Lett.* **2009**, *9*, 4153.
27. Halls, J. J. M.; Pichler, K.; Friend, R. H.; Moratti, S. C.; Holmes, A. B. *Appl. Phys. Lett.* **1996**, *68*, 3120.
28. Wang, Q.; Wang S.; Li, J.; Moriyama, H. J. Polym. Sci., *Part B: Polym. Phys.* **2012**, *50*, 1426.

29. Shaheen, S. E.; Brabec, C. J.; Sariciftci, N. S.; Padinger, F.; Fromherz, T.; Hummelen, J. C. *Appl. Phys. Lett.* **2001**, *78*, 841.
30. Cates, N. C.; Gysel, R.; Dahl, J. E. P.; Sellinger, A.; McGehee, M. D. *Chem. Mater.* **2010**, *22*, 3543.
31. Yu, X.; Xiao, K.; Chen, J.; Lavrik, N. V.; Hong, K.; Sumpter, B. G.; Geohegan, D. B. *ACS Nano* **2011**, *5*, 3559.
32. Grana, E.; Katsigiannopoulos, D.; Avgeropoulos, A.; Goulas, V. *Int. J. Polym. Anal. Charact.* **2008**, *13*, 108.
33. Grana, E.; Katsigiannopoulos, D.; Karantzalis, A. E.; Baikousi, M.; Avgeropoulos, A. *Eur. Polym. J.* **2013**, *49*, 1089.
34. Roncali, J. *Chem. Rev.* **1992**, *92*, 711.
35. Mo, Z.; Lee, K. B.; Moon, Y. B.; Kobayashi, M.; Heeger, A. J.; Wudl, F. *Macromolecules* **1985**, *18*, 1972.
36. Li, C.; Shi, G.; Liang, Y.; Sha, Z. *Polymer* **1997**, *38*, 6421.
37. Lee, J. U.; Jung, J. W. T.; Russell, T. P.; Jo, W. H. *Nanotechnology* **2010**, *21*, 105201.
38. Kim, B. J.; Miyamoto, Y.; Ma, B.; Fréchet, J. M. *Adv. Funct. Mater.* **2009**, *19*, 2273.
39. Heuken, M.; Komber, H.; Erdmann, T.; Senkovsky, V.; Kiriy, A.; Voit, B. *Macromolecules* **2012**, *45*, 4101.
40. Swinnen, A.; Haeldermans, I.; Ven, M.; D'Haen, J.; Vanhoyland, G.; Aresu, S.; D'Olieslaeger, M.; Manca, J. *Adv. Funct. Mater.* **2006**, *16*, 760.
41. Chen, L.; Pang, X. *Nano-Micro Lett.* **2012**, *4*, 30.
42. Motaung, D. E.; Malgas, G. F.; Arendse, C. J. *J. Mater. Sci.* **2011**, *46*, 4942.
43. Malgas, G. F.; Motaung, D. E.; Arendse, C. J. *J. Mater. Sci.* **2012**, *47*, 4282.
44. Nishizawa, T.; Tajima, K.; Hashimoto, K. *Nanotechnology* **2008**, *19*, 424017.
45. Ho, C. S.; Huang, E. L.; Hsu, W. C.; Lee, C. S.; Lai, Y. N.; Lai, W. H. *Jpn. J. Appl. Phys.* **2011**, *50*, 04DK21.
46. Hiorns, R. C.; Cloutet, E.; Ibarboure, E.; Khoukh, A.; Bejbouji, H.; Vignau, L.; Cramail, H. *Macromolecules* **2010**, *43*, 6033.
47. Jayaraman, S.; Rajarathnam, D.; Srinivasan, M. P. *Mater. Sci. Eng. B* **2010**, *168*, 42.
48. Yao, K.; Chen, L.; Hu, T.; Chen, Y. *Organ. Electron.* **2012**, *13*, 1443.
49. Zakhidov, A. A.; Akashi, T.; Yoshino, K. *Synthetic Metals* **1995**, *70*, 1519.
50. Shen, Y.; Zhang, J.; Gu, F.; Xia, Y. *Mater. Chem. Phys.* **2003**, *82*, 401.
51. Hare, J. P.; Kroto, H. W.; Taylor, R. *Chem. Phys. Lett.* **1991**, *177*, 394.
52. Wang, H. S.; Lin, L. H.; Chen, S. Y.; Wang, Y. L.; Wie, K. H. *Nanotechnology* **2009**, *20*, 075201.
53. Bhadra, S.; Singha, N. K.; Khastgir, D. *J. Appl. Polym. Sci.* **2007**, *104*, 1900.
54. Rodrigues, P. C.; Cantao, M. P.; Janissek, P.; Scarpa, P. C. N.; Mathias, A.; Ramos, L. P.; Gomes, M. A. B. *Eur. Polym. J.* **2002**, *38*, 2213.
55. Morita, S.; Zakhidov, A. A.; Kawai, T.; Araki, H.; Yoshino, K. *Jpn. J. Appl. Phys.* **1992**, *31*, L890.
56. Morita, S.; Zakhidov, A. A.; Kawai, T. *Solid State Commun.* **1992**, *82*, 249.
57. Wei, Y.; Tian, J.; MacDiarmid, A.; Masters, J.G.; Smith, A.L.; Li, D. *J. Chem. Soc. Chem. Commun.* **1993**, *7*, 603.
58. Sapurina, I.; Mokeev, M.; Lavrentev, V.; Zgonnik, V.; Trchová, M.; Hlavatá, D.; Stejskal, J. *Eur. Polym. J.* **2000**, *36*, 2321.